DOI: 10.1002/ejic.200801006

Formation of Ho^{III} Trinuclear Clusters and Gd^{III} Monodimensional Polymers Induced by *ortho* and *para* Regioisomers of Pyridyl-Functionalised β-Diketones: Synthesis, Structure, and Magnetic Properties

Philip C. Andrews,[a] Glen B. Deacon,[a] René Frank,[a] Benjamin H. Fraser,[a] Peter C. Junk,*[a] Jonathan G. MacLellan,[a] Massimiliano Massi,[a] Boujemaa Moubaraki,[a] Keith S. Murray,[a] and Morry Silberstein[b]

Keywords: β-Diketonate ligands / Coordination polymers / Cluster compounds / Molecular magnets / Ketones / N,O ligands / Chelates

Reaction of $GdCl_3(H_2O)_6$ and 1,3-bis(pyridin-4-yl)propane-1,3-dione in methanol with an excess of triethylamine produced a monodimensional polymeric chain $[Gd(\textbf{\textit{p}}\textbf{-dppd})_3(H_2O)]_\infty$, whereas treatment of $HoCl_3(H_2O)_6$ with 1,3-bis(pyridin-2-yl)propane-1,3-dione yielded a trinuclear cluster $[Ho_3(\textbf{\textit{o}}\textbf{-dppd})_3(\mu_3\text{-}OH)_2(H_2O)_4Cl_2]Cl_2$. The compounds were characterised by elemental analysis, IR spectroscopy and magnetism, and their structures were investigated by X-ray crystallography. The 8.20-μ_B magnetic-moment value of the polymeric $[Gd(\textbf{\textit{p}}\textbf{-dppd})_3(H_2O)]_\infty$, between 300 and 20 K, and the magnetisation isotherms (2–20 K; fields 0–5 T), are in agreement with essentially uncoupled single-ion Gd^{3+} f^7 centres, a small decrease in μ_{eff} below 20 K being indicative of zero-field splitting. A temperature-dependent dc-susceptibility and magnetisation investigation of the trinuclear (triangular) $[Ho_3(\textbf{\textit{o}}\textbf{-dppd})_3(\mu_3\text{-}OH)_2(H_2O)_4Cl_2]Cl_2$ revealed that spin-orbit and ligand-field effects on the Ho^{3+} centres, leading to thermal depopulation of Zeeman levels and consequent decreases in μ_{eff} values with decreasing temperature, are occurring rather than weak intra-cluster antiferromagnetic coupling. Frequency- and temperature-dependent ac-susceptibility studies on this homometallic Ho^{3+} cluster did not show clear evidence for slow magnetisation reversal, characteristic of single-molecule magnetism (SMM), and this contrasts with such behaviour recently reported, elsewhere, for a Dy^{3+} triangle having the same core structure but with different chelating {*O*,*O*} ligands.

Introduction

Due to the sometimes unpredictable coordination nature of the lanthanoid elements, polynuclear lanthanoid clusters continue to fascinate the synthetic chemistry community. A multitude of structures have been reported in the last decade, the majority of which were obtained serendipitously rather than by a rational synthetic design.[1] These cluster compounds were normally obtained by means of "controlled hydrolysis" of simple lanthanoid salts[2] using a variety of ligands, such as amino acids[1a] and carboxylates,[1e] alkoxides,[3] amides[4] and many more. More recently, methodologies focussed on obtaining specific classes of polynuclear lanthanoid clusters were intensively studied. This impulse was mainly driven in view of the potential applications of these compounds in a wide range of fields such as catalysis,[5] single-molecule magnets,[6] and luminescent materials.[7] The most relevant examples of synthetic design of lanthanoid clusters concern the use of functionalised β-diketones as ligands.[5,8] The general method consists of treating a mixture of a lanthanoid salt and the relevant diketone ligand with an excess of triethylamine in methanol. The base serves to deprotonate both the ligand and the water molecules coordinated to the metal centre, thus initiating the formation of hydroxo-bridged polynuclear species encapsulated in a shell of β-diketonate ligands. Depending on the relative size of both the ligand and the lanthanoid cation, this synthetic procedure yielded the formation of dimeric,[9] tetranuclear,[8,10] pentanuclear,[5,10c] nonanuclear,[11] dodecanuclear,[12] and tetradecanuclear[7c] lanthanoid hydroxo diketonate clusters.

As part of our work related to the synthesis and characterisation of polynuclear lanthanoid hydroxo clusters, we have prepared β-diketones functionalised with pyridine rings bearing the nitrogen atom either in position 2′ or 4′, namely 1,3-bis(pyridin-2-yl)propane-1,3-dione (***o*-dppd**H) and 1,3-bis(pyridin-4-yl)propane-1,3-dione (***p*-dppd**H) (Scheme 1). We therefore attempted the preparation of clusters by treatment of lanthanoid chloride salts with either ***o***-

[a] School of Chemistry, Monash University,
Melbourne, Victoria 3800 Australia
E-mail: peter.junk@sci.monash.edu.au
[b] School of Medicine Nursing and Health Sciences, Monash University,
Melbourne, Victoria 3800 Australia

Supporting information for this article is available on the WWW under http://www.eurjic.org or from the author.

dppdH or ***p*-dppd**H in methanol in a 1:2 ratio with an excess of base. From $GdCl_3(H_2O)_6$ and $HoCl_3(H_2O)_6$ two new structurally characterised compounds have been obtained: the monodimensional polymer $[Gd(\textbf{\textit{p}-dppd})_3(H_2O)]_\infty$ (**1**) and the trinuclear cluster $[Ho_3(\textbf{\textit{o}-dppd})_3(\mu_3\text{-}OH)_2(H_2O)_4Cl_2]Cl_2$ (**2**). The latter is a novel structure in lathanoid hydroxo diketonate cluster chemistry, although this trinuclear cage motif has been known to form using other different classes of ligands, e.g. hydrido and funtionalised pyridines,[4] vanillin,[6c,6f] and aryl oxides.[3c,3d] The results herein demonstrate how simple regio-control of the position of the extra donor atom in the β-diketonate ligands allows templating of the resulting structure. The magnetic properties of the compounds are also described in some detail and comparisons are made, for **2** with recent studies on a structurally related trinuclear Dy^{III} cluster.[6c]

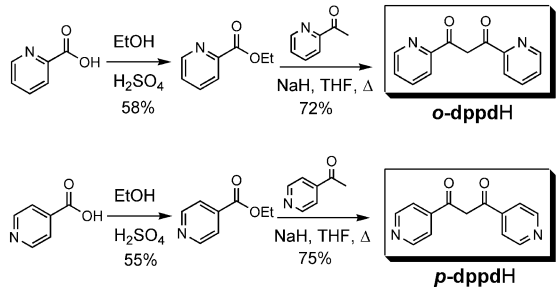

Scheme 1. Synthetic pathway for the ligands *o*-**dppd**H and *p*-**dppd**H.

Results and Discussion

Synthesis and Characterisation of the Polymer 1 and Trinuclear Cluster 2

The ligands ***o*-dppd**H and ***p*-dppd**H were synthesised following a modified literature procedure,[13] as reported in Scheme 1. They were prepared by the Claisen condensation between the ethyl esters of picolinic acid or isonicotinic acid and the corresponding 2-acetylpyridine or 4-acetylpyridine. Both reactions were carried out in dry THF, using NaH to generate the corresponding sodium enolates in the presence of the esters. The method does not require the generation of a base in situ as an extra step, such as sodium ethanoate in toluene, and works efficiently in conditions that are not strictly anhydrous.

Treatment of a mixture of 1 equiv. of $GdCl_3(H_2O)_6$ and 2 equiv. of ***p*-dppd**H in methanol with an excess of triethylamine yielded the monodimensional polymer **1** (Scheme 2). Although the stoichiometry of the reaction was set to a metal/ligand ratio of 1:2 in order to form a polynuclear cluster, a trisubstituted complex, which polymerised by the ligand pyridyl nitrogen, was instead obtained. Rather than performing the reaction at room temperature, we used reflux conditions as it was previously observed that the clusters were the thermodynamically favoured products. The crude product was added to a 1:10 mixture EtOH/H_2O where it precipitated out leaving in solution any unreacted ligand and Gd salt. The compound was then dissolved in ethanol and vapour diffusion of hexane into the solution produced suitable crystals for X-ray diffraction. The compound was analysed by means of elemental analysis and IR spectroscopy. Elemental analysis on the bulk sample reveals the presence of four extra water molecules in the lattice, some of which are replaced by ethanol when crystals are grown from the ethanolic solution. Hydration of the product was confirmed by the broad IR band at 3500–2500 cm^{-1}, and the band at 1514 cm^{-1} was attributed to the C=O bond in the diketonate ligand.

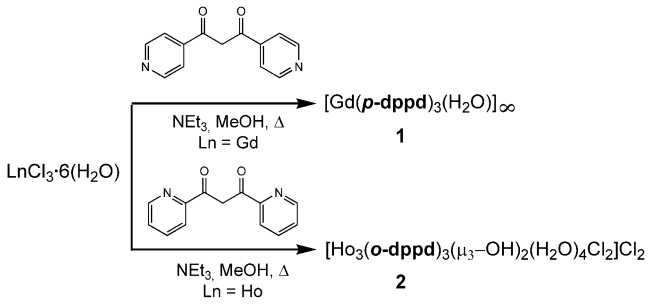

Scheme 2. Synthetic pathway for the polymer **1** and the cluster **2**.

Treatment of a mixture of 1 equiv. of $HoCl_3(H_2O)_6$ and 1 equiv. of ***o*-dppd**H in methanol with an excess of triethylamine yielded a trinuclear cage **2** (Scheme 2). The same conditions for the preparation of **1** were used. Due to the polar and ionic nature of the cluster, the usual extraction of the product by toluene or dichloromethane was not possible.[10] Therefore, the unreacted ***o*-dppd**H ligand was removed by washing the crude product with acetonitrile, whereas any unreacted Ho salts were removed by dissolving the compound in pyridine and filtering off any undissolved residue. After this treatment, we were able to obtain suitable crystals for X-ray diffraction by slow evaporation of a methanol solution of **2**. The compound was again analysed by means of elemental analysis and IR spectroscopy. Elemental analysis shows loss of all lattice solvent molecules from the bulk after several hours under reduced pressure. The C=O band is shifted to 1519 cm^{-1}, with respect to the usual values of C=O double bonds, due to the partial double bond character of the diketonate carbonyl group.

X-ray Crystal Structures

Figure 1 shows the molecular structure of polymer $[Gd(\textbf{\textit{p}-dppd})_3(H_2O)]_\infty$ (**1**) which crystallises in the monoclinic space group $P2_1/c$. The polymer is composed of linear chains of trisubstituted neutral complexes. Overall the Gd centres are octacoordinate, bonded by three chelating (*O*,*O*′) diketonate groups, one water molecule and a bridging pyridyl-N atom from another unit. Gd–O(diketonate) bonds are slightly asymmetrical but lie within the expected range for this type of interaction ($short_{ave}$ 2.33 Å and $long_{ave}$ 2.39 Å, Table 1). Internal ligand O–Gd–O bite angles vary little, ranging from 70.38(14)–71.47(12)°. The water molecule binds to the Gd at a distance of 2.380(4) Å and

lies *trans* to the interaction of ligand 2 with the Gd centre [the $(H_2)O$–Gd–C(H) angle is 175.53(15)°] but essentially within the [O(3)–Gd–O(4)] plane (RMS deviation from planarity for all four atoms is 0.0087 Å). The respective planes of ligands 1 and 3 with Gd form angles of 80.68(14)° and 86.72(14)° on either side of the (ligand 2)–Gd–$O(H_2)$ plane and at an angle of 158.86(22)° to each other. The overall chain-structure is linked together by N(pyridyl)–Gd bonds of 2.624(4) Å with four near identical angles to the closest Gd–O bond of each ligand and to the water molecule [range of angles 71.11(13)°–73.85(13)°]. Although the polymeric chains are unidimensional, they are interlocked through intermolecular face-to-face π-stacking. Two symmetry-generated rings align above and below the ring containing N(1) with average distances between adjacent pyridyl rings of 3.51 Å [to ring containing N(6)*] and 3.67 Å [to ring containing N(5)**]. Moreover, the water molecule bound to the Gd centre completes a hydrogen-bonded network through interactions with the pyridyl-N atoms of two parallel, neighbouring chains, N(3) and N(1) as shown in Figure 2. Cavities within the network are filled by two solvent molecules per monomeric unit. One is occupied by an ethanol molecule, disordered over two positions with equal occupancies, and the second is occupied by ethanol or water (major component of disorder 80% EtOH). One pyridyl substituent on each of the β-diketonate ligands is disordered over two positions (refined occupancy of major component: 68.3%, 76.5% and 80.0% for ligands 1, 2 and 3, respectively). The two disordered components of ligand 3 also account for the site disorder of the neighbouring lattice solvent EtOH(major)/H_2O(minor) mentioned previously. The disorder was allowed to freely refine to near 80% and was then fixed at this value for all further refinements. The donor–acceptor distances involved in the hydrogen bonding network are 2.770(8) Å for O(7)···N(3)* [2.66(2) Å for O(7)···N(3A)*; the minor component of disorder] and 2.727(6) Å for O(7)···N(1)*. There is one further weak H-bond involving the disordered ethanol, O(9)···N(5), at 2.905(14) Å. There is no significant bonding to the other component of this disorder when the ethanol is oriented in the opposite direction.

Compound $[Ho_3(\textbf{\textit{o}-dppd})_3(\mu_3\text{-}OH)_2(H_2O)_4Cl_2]Cl_2$ (**2**) crystallises in the triclinic space group $P\bar{1}$ and is reported in Figure 3 and Table 2. This novel trinuclear complex shows remarkable differences from its previous β-diketonate cluster analogues, and these can be ascribed to the addition (and position) of a donor N atom in the pyridyl diketonate ligand. Unlike its regioisomer in **1** (***p*-dppd**H), the position of the N in ***o*-dppd**H allows intramolecular donation which results in the formation of this unusual arrangement. Each diketonate ligand binds to two Ho atoms through $\mu\text{-}\eta^2(N,O);\eta^2(O,O')$ bonding, leaving one pyridyl-N atom per ligand free. One O per ligand [O(2,4,6)] forms a planar six-membered central ring with the three Ho centres, RMS deviation of fitted atoms 0.0146 Å (RMS deviation of fitted atoms when both ligand O atoms and the coordinated N are included is 0.1861 Å). The three Ho^{3+} centres form an equilateral triangle, as evidenced by the Ho–Ho distances

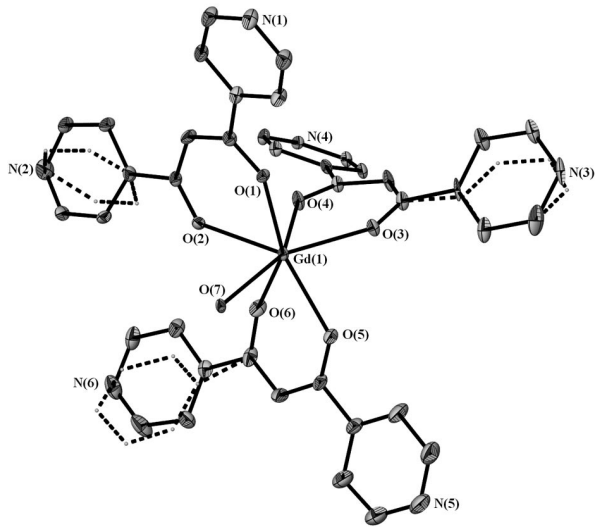

Figure 1. Molecular structure of complex **1** showing 30% ellipsoids with all H atoms and lattice solvent molecules removed.

Table 1. Selected bond lengths [Å] and angles [°] for **1**.

Gd(1)–O(1)	2.335(4)	Gd(1)–O(5)	2.408(4)
Gd(1)–O(2)	2.387(4)	Gd(1)–O(6)	2.327(4)
Gd(1)–O(3)	2.368(4)	Gd(1)–O(7)	2.380(4)
Gd(1)–O(4)	2.338(4)	Gd(1)–N(4)*	2.624(4)
O(1)–Gd(1)–O(2)	71.13(12)	O(6)–Gd(1)–O(7)	82.85(15)
O(3)–Gd(1)–O(4)	71.47(12)	O(1)–Gd(1)–N(4)*	71.11(13)
O(5)–Gd(1)–O(6)	70.38(14)	O(2)–Gd(1)–N(4)*	126.31(13)
O(1)–Gd(1)–O(7)	94.05(14)	O(3)–Gd(1)–N(4)*	73.85(13)
O(2)–Gd(1)–O(7)	74.59(13)	O(4)–Gd(1)–N(4)*	138.97(13)
O(3)–Gd(1)–O(7)	142.28(13)	O(5)–Gd(1)–N(4)*	73.81(13)
O(4)–Gd(1)–O(7)	146.22(13)	O(6)–Gd(1)–N(4)*	138.86(15)
O(5)–Gd(1)–O(7)	80.07(14)	O(7)–Gd(1)–N(4)*	71.54(13)

* Symmetry transformation used to generate equivalent atoms: $x + 1, y, z$

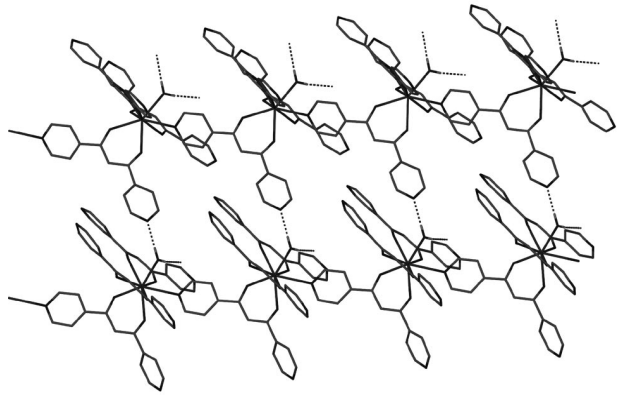

Figure 2. Polymeric structure of complex **1** with all H atoms removed except those on the attached water molecule.

and corresponding angles in Table 3. Each β-diketonate ligand again binds asymmetrically to the Ho centres. One O atom per ligand [O(2,4,6)] bridges between two Ho atoms to form the central $(HoO)_3$ ring with an average Ho–O bond length of 2.36 Å. The second oxygen atom per ligand

[O(1,3,5)] bonds to only one Ho atom with a marginally shorter bond length, averaging 2.30 Å, reflecting the lower connectivity of two for the O atoms. The bonding pyridyl-N atoms [N(2,4,6)] of each ligand have nearly identical Ho–N bond lengths; range 2.505(11) Å–2.512(10) Å. Intraligand O–Ho–O bite angles for Ho(1), Ho(2) and Ho(3) are 71.7(3), 72.8(3) and 73.1(3)° respectively with O–Ho–N angles of 65.3(3), 64.7(3) and 65.0(3)°. As shown in Figure 4, the two hydroxy O atoms lie perpendicular to the centre of the $(HoO)_3$ ring [distances above and below the centroid are 1.191 Å to O(7) and 1.208 Å to O(8)] with the six Ho–O(H) distances ranging from 2.355(9) Å–2.394(8) Å. Unusually not all the chloride anions are displaced from the Ho centres by the hydroxo ligands, a feature not displayed by any of the previously reported β-diketonate clusters.[5,7c,8–12] Two Ho cations, Ho(1) and Ho(3) are connected to different Cl atoms in the first coordination sphere at distances of 2.670(3) Å and 2.585(6) Å respectively. All three metals are octacoordinate with their coordination spheres being completed by either one [or two in the case of Ho(2)] molecules of water with average Ho–O distances of 2.34 Å. This trinuclear cluster possesses an overall 2+ charge and it is counterbalanced by two more distant Cl^- anions which are not in close contact with any of the metal centres [the closest Ho···Cl distance is 4.5744(42) Å].

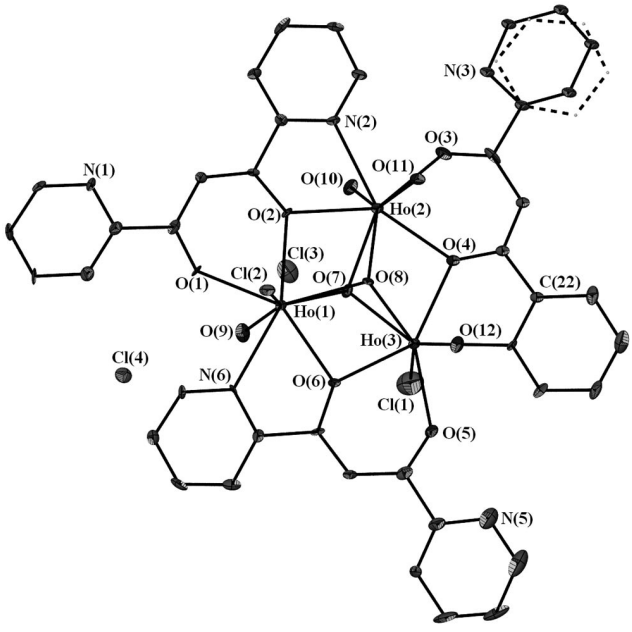

Figure 3. Molecular structure of cluster **2** showing 30% ellipsoids with all H atoms and lattice solvent molecules removed.

Large solvent-accessible voids within the lattice are occupied by five distinct molecules of water and one further water molecule which is disordered with a molecule of methanol. This disorder freely refined to 50% occupancies of the respective fragments and was therefore constrained at this value for all further refinements. The lattice solvents, together with the two chloride counteranions, form an extended hydrogen-bonded network which can be seen in Figure 4 and relevant distances are given in Table 4. The hydrogen bonding is located above and below the Ho_3 plane, where either face of the molecule is free of the steric hindrance of the pyridyl rings. The presence of free faces in the molecular structure is also unusual behaviour in diketonate cluster chemistry, as in previously reported structures the polymetallic core has always been completely surrounded by the organic ligands.[9,10,12] As previously stated, all the molecular units are arranged with their Ho_3 planes parallel. In addition to the hydrogen-bonded network, intermolecular π-stacking (perpendicular to the plane of the molecule) occurs between either the delocalised backbone of the diketonate moiety and a pyridyl ring or between two pyridyl rings. We located 32 unique contacts from six different π-stacking arrangements with distances below 3.9 Å and averaging 3.649 Å. There is no lateral interaction parallel to the Ho_3 plane, as seen in **1**, despite the presence of one unbound pyridyl-N atom per diketonate ligand. In two of the unbound rings the free N atoms [N(3) and N(5)] face "inwards" in the same direction as the coordinated N atoms. In the other ligand, N(1) faces away from the central core and H-bonds to the C–H on the β-diketonate backbone of the same ligand, C(1)···N(1), with a distance of 2.884(17) Å.

Table 2. Selected bond lengths [Å] and angles [°] for **2**.

Ho(1)–O(1)	2.300(8)	Ho(2)–O(8)	2.394(8)
Ho(1)–O(2)	2.351(8)	Ho(2)–O(10)	2.337(8)
Ho(1)–O(6)	2.371(9)	Ho(2)–O(11)	2.325(8)
Ho(1)–O(7)	2.378(8)	Ho(2)–N(2)	2.505(11)
Ho(1)–O(8)	2.376(8)	Ho(3)–O(4)	2.360(8)
Ho(1)–O(9)	2.362(9)	Ho(3)–O(5)	2.290(9)
Ho(1)–N(6)	2.506(10)	Ho(3)–O(6)	2.318(8)
Ho(1)–Cl(2)	2.670(3)	Ho(3)–O(7)	2.371(8)
Ho(2)–O(2)	2.354(8)	Ho(3)–O(8)	2.363(8)
Ho(2)–O(3)	2.317(10)	Ho(3)–O(12)	2.346(8)
Ho(2)–O(4)	2.327(9)	Ho(3)–N(4)	2.512(10)
Ho(2)–O(7)	2.355(9)	Ho(3)–Cl(1)	2.585(6)
O(1)–Ho(1)–O(2)	71.7(3)	O(12)–Ho(3)–Cl(1)	146.4(3)
O(8)–Ho(1)–O(7)	60.6(3)	Ho(1)–O(2)–Ho(2)	97.7(3)
O(6)–Ho(1)–N(6)	65.3(3)	Ho(2)–O(4)–Ho(3)	98.1(3)
O(9)–Ho(1)–Cl(2)	146.7(3)	Ho(3)–O(6)–Ho(1)	98.6(3)
O(3)–Ho(2)–O(4)	72.8(3)	Ho(2)–O(7)–Ho(3)	97.1(3)
O(7)–Ho(2)–O(8)	60.6(3)	Ho(2)–O(7)–Ho(1)	97.0(3)
O(2)–Ho(2)–N(2)	64.7(3)	Ho(3)–O(7)–Ho(1)	97.0(3)
O(10)–Ho(2)–O(11)	146.7(3)	Ho(3)–O(8)–Ho(1)	97.3(3)
O(5)–Ho(3)–O(6)	73.1(3)	Ho(3)–O(8)–Ho(2)	96.2(3)
O(8)–Ho(3)–O(7)	60.8(3)	Ho(1)–O(8)–Ho(2)	96.0(3)
O(4)–Ho(3)–N(4)	65.0(3)		

Table 3. Ho–Ho distances [Å] and corresponding angles [°] in the triangular core of **2**.

Ho(1)–Ho(2)	3.5435(15)
Ho(1)–Ho(3)	3.5560(18)
Ho(2)–Ho(3)	3.5409(14)
Ho(2)–Ho(1)–Ho(3)	59.84(3)
Ho(1)–Ho(2)–Ho(3)	60.26(4)
Ho(2)–Ho(3)–Ho(1)	59.91(3)
O(7)–O(8) 2.398(11)	2.398(11)

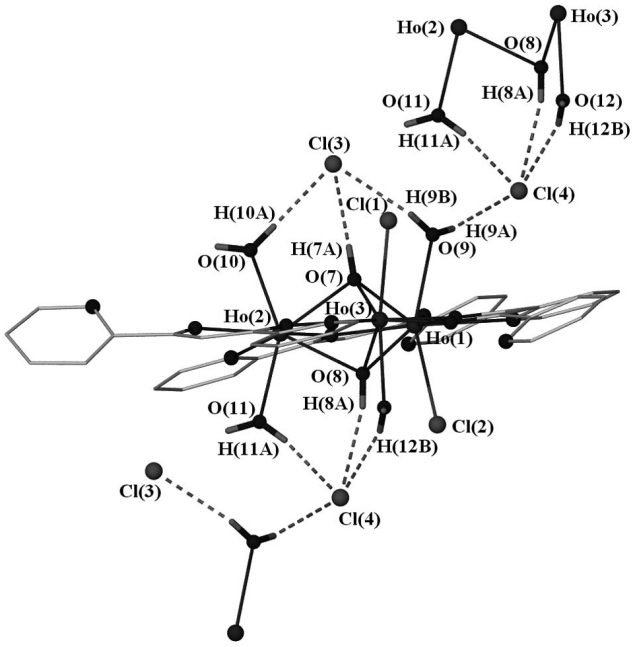

Figure 4. Molecular structure of cluster **2** showing H-bonding network.

Table 4. Hydrogen bonds distances [Å] for **2**.

D–H···A	*d*(H···A)	*d*(D···A)
O(11)–H(11B)···O(14)	1.85(7)	2.650(13)
O(10)–H(10A)···Cl(3)	2.21(3)	3.036(10)
O(7)–H(7A)···Cl(3)	2.46(10)	3.248(9)
O(10)–H(10B)···O(16)	1.96(6)	2.781(16)
O(9)–H(9B)···Cl(3)	2.42(14)	3.120(10)
O(9)–H(9A)···Cl(4)	2.44(8)	3.206(10)
O(11)–H(11A)···Cl(4)*	2.24(4)	3.056(9)
O(12)–H(12B)···Cl(4)*	2.27(4)	3.036(10)
C(1)–H(1)···N(1)	2.55	2.884(17)

* Symmetry transformations used to generate equivalent atoms: $x + 1, y, z$

The striking feature of both structures is represented by the fact that the pyridine nitrogen atoms are able to displace oxygen donor ligands, most likely water or hydroxide. Although lanthanoid cations have a marked preference for oxygen from H_2O and OH^- (especially in non-anhydrous environments) we have in fact encountered in our studies a similar preference for weaker donors, where lanthanoid cations form a rod-like metal-organic framework coordinating neutral diols or amines, which is induced by heating the lanthanoid complex in water.[14]

Magnetic Properties

Complex **1** has a room-temperature magnetic moment of 8.20 μ_B ($\chi_M T$ = 8.40 $cm^3 mol^{-1} K$) which is a little higher than values normally observed for mononuclear Gd^{3+} compounds that generally display close to free-ion f^7 (orbitally non degenerate $^8S_{7/2}$ ground state) behaviour for which the expression $g[J(J + 1)]^{0.5}$ yields 7.94 μ_B ($\chi_M T$ = 7.88 $cm^3 mol^{-1} K$). To probe for any spin-spin coupling through the long intra-chain ligand-bridging pathways or the H-bonded inter-chain pathways (Figure 2), anticipated to be very weak or zero, measurements of μ_{eff} were made down to 2 K, in a field of 1 T. In Figure 5 it can be seen that the moments remain independent of temperature down to ca. 20 K, then decrease rapidly to reach 6.77 μ_B ($\chi_M T$ = 5.73 $cm^3 mol^{-1} K$) at 2 K, the decrease probably being due to zero-field splitting of the $^8S_{7/2}$-derived ligand-field ground state rather than to very weak antiferromagnetic coupling, 2*J* values for the latter being usually observed in the range – (0.04 to 0.21 cm^{-1}) even when better superexchange-pathway ligands than ***p*-dppd** are present.[15] The corresponding plot of χ_M^{-1} vs. temperature, for **1**, is essentially Curie-like with C = 9.0 $cm^3 mol^{-1} K$ and θ = –0.83 K (Figure 5), again indicative of monomer-like behaviour but such C and θ values have often been ascribed to weak antiferromagnetic coupling.[15] Magnetisation isotherms, measured between 2 and 20 K under fields of 0 to 5 T (Supporting Information), further confirm this situation, the 2 K plot showing near saturation with M = 8.2 $N\mu_B$ in the 5 T field, a value a bit higher than normal for a S = 7/2 system.

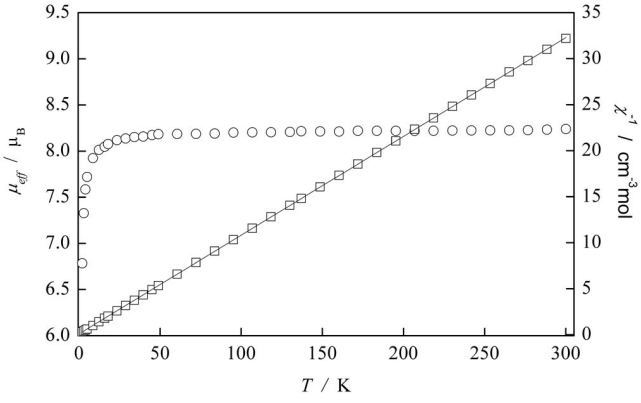

Figure 5. Plot of effective magnetic moment (o) and χ_M^{-1} (□) vs. temperature, per Gd, for **1**, in a field of 1 Tesla. The solid line is fitted to the Curie–Weiss Law using the parameters given in the text.

The plot of effective magnetic moment, per Ho_3, vs. temperature for complex **2** is given in Figure 6. The applied dc field was 1 T. There is a gradual decrease in μ_{eff} from 17.83 μ_B ($\chi_M T$ = 39.74 $cm^3 mol^{-1} K$) [μ_{eff} per Ho = 10.31 μ_B] at 295 K to ca. 17 μ_B at 100 K, then more rapidly to reach 8.89 μ_B ($\chi_M T$ = 9.88 $cm^3 mol^{-1} K$) [μ_{eff} per Ho = 5.14 μ_B] at 2 K. Use of a 0.1 T field in the region 70–2 K showed essentially the same μ_{eff} values, apart for small differences at 2 K, as did the 1 T data indicating that field induced crossing of the lowest levels is minimal in this case. The Ho^{3+} f^{10} configuration, with a $^5I_8$ free-ion ground state, typically leads to observed values of ca. 10.4 μ_B in monomeric systems, and this compares well to the calculated $g[J(J + 1)]^{0.5}$ value of 10.6 μ_B. Thus the ligand-field (Stark) levels emanating from the spin-orbit J = 8 ground level are populated at room temperature. The next higher J level is at energy much greater than kT. We have not made quantitative calculations of ligand-field splittings in the present distorted eight-coordinate geometry, but early calculations by Lea et

al.[16a] showed that a ligand field of cubic symmetry produced splittings into a singlet, two non-magnetic doublets and four triplets. The observed decrease in μ_{eff} values with decreasing temperature, for **2**, strongly suggests that the decrease is due to thermal depopulation of the low-lying Zeeman levels originating from the above-mentioned ligand-field levels, and is not due to weak antiferromagnetic coupling. Indeed, very similar values of μ_{eff}, per Ho, were observed for a monomeric Ho^{III} complex even at the 2 K region where the effects of any magnetic exchange coupling would be noted.[16b] The apparent lack of exchange coupling in **2** contrasts with the weak antiferromagnetic coupling noted in a Gd^{III} cluster[6f] and the non-collinear Ising-like antiferromagnetic exchange observed in a Dy^{III} cluster,[6d,6e] both of which have the same $[M_3L_3(\mu_3\text{-}OH)_2]$ core structure as in **2**. The Dy^{III} compound has yielded a very interesting non-magnetic ground state system as well as, surprisingly, slow relaxation of the magnetisation, the latter originating from low lying excited magnetic states.[6d,6e,6f]

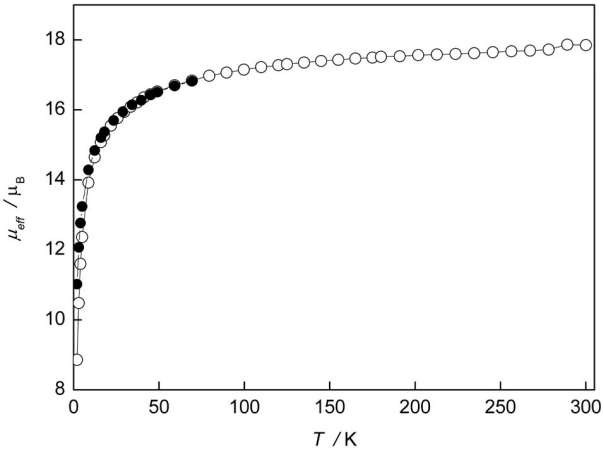

Figure 6. Plot of effective magnetic moment (o) vs. temperature, per Ho_3, for **2**, in a field of 1 Tesla [the data in a field of 0.1 Tesla (●) are also shown]. The solid lines are guides to the eye and are not fitted curves.

In order to probe further the low-lying Zeeman energy levels in **2**, the magnetisation (M) isotherms were determined in fields up to 5 T, over the temperature range 2–20 K, the data being shown in Figure 7. It can be seen that at the lowest temperature of 2 K, and highest field of 5 T, the M value is 15.65 $N\mu_B$ and far from being saturated. Indeed, the 3, 4 and 5.5 K values, in the 5 T field, are close to the value at 2 K, such behaviour normally, in d-block clusters, indicating that low-lying levels are close to the ground level and that Zeeman population effects, and/or zero-field splitting effects, are playing a part. A spin-only value of S, for three Ho^{3+} ions, would be close to 12 $N\mu_B$ but this ignores the orbital (L) contribution, and, as in recent pentanuclear and trinuclear Dy^{III} (single-ion spin of 5/2) cluster,[6a,6c] the observed 2 K/5 T value of M, in **2**, is higher than the spin-only value. The shapes of the magnetisation curves at temperatures 2–5.5 K are consistent with closely spaced Zeeman levels from single-ion Ho^{III} centres, the 2 K curve being very similar to that reported for a Ho^{III} monomer.[16b] Any antiferromagnetic coupling, within the trinuclear cluster must be very weak at best. What is clear is that there is no maximum in χ_M and no rapid S-shaped rise in M, prior to saturation (above 2 T) of the kind recently found in the Dy triangular analogue.[6c]

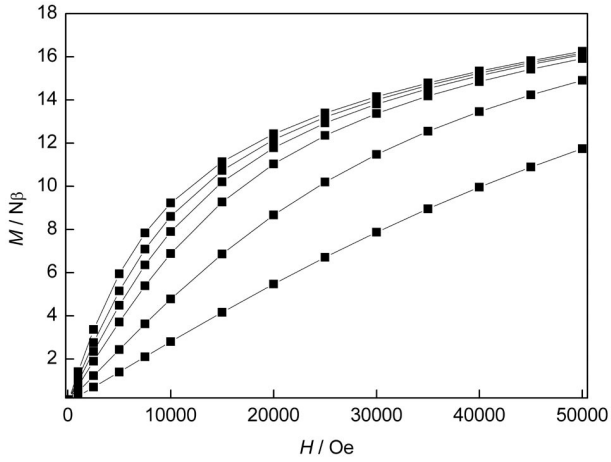

Figure 7. Plots of isothermal magnetisation, per Ho_3, at temperatures of 2 (top), 3, 4, 5.5, 10 and 20 K (bottom). The solid lines are just guides to the eye and are not calculated plots. (Note that 1 T = 10000 Oe).

To probe for possible single-molecule magnetic behaviour (SMM) in **2** we measured the (dynamic) ac in-phase χ_M' susceptibilities and out-of-phase χ_M'' values, as a function of frequency (50 to 1500 Hz), between 10 and 2.4 K. Very weak frequency-dependent χ_M'' values were noted in the 4–2 K region, at the temperature limit of the instrument but no firm conclusions can be drawn from this in the absence of data below 2 K. Further, the frequency dependence was barely detectable in the χ_M' plot, the latter showing Curie–Weiss behaviour as in the dc plot in this low-temperature region.

Conclusions

In summary we have shown in this work how the introduction of an extra nitrogen donor atom in dipyridyl β-diketone ligands has favoured the formation of either lanthanoid polymeric or hydroxo cluster species. The type of product obtained is efficiently templated by the position of the pyridine nitrogen. When the nitrogen is in position 2′, a novel trinuclear hydroxo cluster is obtained, whereas nitrogen in position 4′ induces the formation of a monodimensional polymer. Despite the high oxophilic nature of lanthanoid cations, coordination of the pyridine rings is made possible by performing the reactions in refluxing conditions rather than room temperature. Magnetic susceptibility and magnetisation studies, using dc and ac methods, reveal an absence of spin-spin coupling in **1** and **2**, the data for the trinuclear cluster, **2**, being explainable in terms of the low-lying energy levels originating from spin-orbit and ligand-field splittings of the constituent Ho^{III} single ions, with any antiferromagnetic exchange contribution being

close to zero. The magnetic behaviour of **2** is markedly different to the non-collinear Ising exchange recently observed for a Dy^{III} cluster having the same core and bridging motif, but with a different O-bridging chelator than ***o*-dppd**$^-$. It is likely that magnetic anisotropy differences between the Ho^{III} and Dy^{III} centres will influence the spin structure in the triangular core of the cluster as well as the relative magnitudes of ligand-field and magnetic-exchange contributions.

Experimental Section

General: All solvents and reagents were purchased from Aldrich and used as received unless otherwise specified. THF was dried prior to use with a M-Braun MB SPS-800 purification system. Ethyl picolinate and ethyl isopicolinate were prepared according to previously published procedures.[17] ^{1}H NMR spectra were recorded at 200 MHz with a Bruker AC 200 spectrometer. ^{13}C NMR spectra were recorded in the DEPT mode, proton broad band decoupled at 50 MHz with a Bruker AC 200 spectrometer. All the spectra were referenced using the solvent signal. Electrospray ionisation spectra (ESI) were generated with a Micromass Platform II QMS spectrometer. Electron impact spectra (EI) were recorded with a Shimadzu QP5050A GCMS system. Attenuated total reflection (ATR) spectra were obtained with a Bruker Equinox 55 spectrometer, equipped with a Specac Diamond ATR source. Elemental microanalyses were performed by the Campbell Microanalytical Laboratory (Department of Chemistry, University of Otago, Dunedin, New Zealand). Melting points were measured with a Stuart Scientific melting point apparatus SMP3 in an open capillary. Magnetic measurements were carried out using a Quantum Design MPMS 5 Squid magnetometer (for dc susceptibilities and magnetisations), and a Quantum Design PPMS instrument with an ac susceptibility attachment (for ac in-phase and out-of-phase susceptibilities) as described previously.[18] Crystalline samples of compounds **1** and **2** were mounted upon glass fibres in highly viscous oil at 123(2) K and data were collected with an Enraf–Nonius Kappa CCD diffractometer [graphite-monochromated Mo-K_α X-ray radiation (λ = 0.71073 Å)] and corrected for absorption using the SORTAV[19] package. The SHELX[20] suite of programs was employed for structural solution and refinements using the graphical interface X-Seed.[21] For compound **1**, each of the pyridyl substituents of the β-diketonate ligands were modelled as disordered over two positions (refined occupancy of major component: ligand A 68.37%, ligand B 76.64% and constrained for ligand C 80.00%). The two disorder components for ligand C also related to a site disorder of a neighbouring lattice solvent EtOH(major)/H_2O-(minor). A second lattice solvent molecule of ethanol was present and disordered over two positions with equal occupancies. The minor components of disorder within the main residue and the lattice solvent were refined isotropically. In compound **2** one pyridyl substituent was disordered over two sites (refined occupancy of major component 64.38%) and one lattice molecule of methanol was disordered with a molecule of water with equal occupancies. Neither of these molecules nor the minor component of the pyridyl disorder could sustain anisotropic refinement and were therefore refined isotropically. The solvent accessible voids in the structure almost certainly contained molecules of water however we were unable to model them satisfactorily with the current data.

Synthesis of the Diketones *o*-dppdH and *p*-dppdH: 2-Acetyl- or 4-acetylpyridine (5.00 g, 41.3 mmol) was dissolved in 200 mL of anhydrous THF and NaH (60% dispersion in paraffin oil, 2.00 g, 50.0 mmol) was carefully added. Then, the corresponding ethyl picolinate or ethyl isopicolinate (6.24 g, 41.3 mmol) was added and the mixture was vigorously stirred and heated at 60 °C for 12 h. More portions of THF were added as the mixture thickened. The solvent was eventually removed under reduced pressure and the resulting solid was added to a 1:5 mixture of glacial acetic acid and water. The remaining solid was filtered and recrystallised from methanol.

1,3-Bis(pyridin-2-yl)propane-1,3-dione (*o*-dppdH): Yield 6.72 g (72%), m.p. 100–101 °C. ^{1}H NMR (200 MHz, [D_6]acetone, diketone tautomer, only small traces of enol tautomer are present in the spectrum): δ = 4.89 (s, 2 H), 7.61 (ddd, J = 7.6, J = 4.7, J = 1.3 Hz, 2 H), 8.04 (td, J = 7.6, J = 1.7 Hz, 2 H), 8.18 (ddd, J = 7.6, J = 1.0 Hz, 2 H), 8.78 (m, 2 H) ppm. ^{13}C NMR (50 MHz, [D_6]-DMSO, diketone tautomer, only small traces of enol tautomer are present in the spectrum): δ = 48.01, 121.86, 127.85, 137.75, 149.68, 151.88, 196.57 ppm. IR (Diamond ATR): $\tilde{\nu}$ = 3136 (w), 3050 (w), 2995 (w), 2922 (w), 2852 (w), 1650 (s), 1577 (s), 1550 (s), 1241 (s), 1279 (s), 736 (s) . cm^{-1} MS (ESI): calcd. for $C_{13}H_{11}N_2O_2$ [MH^+] 227.0; found 227.0.

1,3-Bis(pyridin-4-yl)propane-1,3-dione (*p*-dppdH): Yield 7.01 g (75%), m.p. 156–157 °C. ^{1}H NMR (200 MHz, [D_6]acetone, enol tautomer, only small traces of the diketone tautomer are present in the spectrum): δ = 7.46 (s, 1 H), 8.03 (d, J = 2.9 Hz, 4 H), 8.84 (d, J = 2.9 Hz, 4 H) ppm. ^{13}C NMR (50 MHz, [D_6]acetone, enol tautomer, only small traces of the diketone tautomer are present in the spectrum): δ = 95.93, 121.46, 142.43, 151.75, 185.56 ppm. IR (Diamond ATR): $\tilde{\nu}$ = 3095 (w), 3035 (w), 1611 (s 1579 s), 1539 (s), 1408 (s), 1368 (m), 1278 (m), 783 (s) . cm^{-1}. MS (ESI): calcd. for $C_{13}H_{11}N_2O_2$ [MH^+] 227.0; found 227.1.

{[Gd(*p*-dppd)$_3$(H$_2$O)]·4(H$_2$O)}$_\infty$ (1): $GdCl_3·6H_2O$ (0.50 g, 1.4 mmol) and ***p*-dppd**H (0.61 g, 2.7 mmol) were dissolved in 100 mL MeOH. NEt_3 (1.8 mL, 13.2 mmol) was added dropwise to the solution, which was refluxed for 48 h. The solvent was finally evaporated and the resulting solid was added to a 1:10 EtOH/H_2O mixture (50 mL). The leftover solid was filtered off and dried under reduced pressure yielding the title compound as a yellow solid. Yield 0.83 g (67%). Crystals suitable for X-ray diffraction could be obtained by diffusion of n-hexane into an ethanolic solution of the title compound after several days. IR (Diamond ATR): $\tilde{\nu}$ = 2500–3500 [s (br)], 3034 (w), 1591 (s), 1538 (s), 1514 (s), 1421 (m), 1392 (s), 772 (m) cm^{-1}. $C_{39}H_{37}GdN_6O_{11}$: calcd. C 50.75, H 4.04, N 9.11; found C 51.05, H 3.87, N 8.87. Magnetic moment at 295 K, μ_{eff} = 8.20 μ_B.

{[Ho$_3$(*o*-dppd)$_3$(μ_3-OH)$_2$(H$_2$O)$_4$Cl$_2$]Cl$_2$} (2): $HoCl_3·6H_2O$ (0.84 g, 2.2 mmol) and ***o*-dppd**H (1.00 g, 4.4 mmol) were dissolved in 100 mL MeOH. NEt_3 (3.0 mL, 21.5 mmol) was then added dropwise and the solution was heated to reflux for 24 h. The solvent was removed under reduced pressure and 80 mL of acetonitrile were added to the crude product. The leftover solid was filtered off and subsequently dissolved in pyridine. The mixture was filtered again and pyridine was removed from the filtrate under reduced pressure yielding the title compound as a brown crystalline solid. Yield 0.78 g (70%). Needle shape crystals suitable for X-ray diffraction were harvested from slow evaporation of a MeOH solution after a few days. IR (Diamond ATR): $\tilde{\nu}$ = 2500–3500 [s (br)], 1607 (m), 1593 (m), 1580 (m), 1562 (m), 1519 (s), 1444 (s), 1395 (s), 765 (m) cm^{-1}. $C_{39}H_{37}Cl_4Ho_3N_6O_{12}$: calcd. C 33.03, H 2.63, N 5.93; found C 33.45, H 2.86, N 5.60. Magnetic moment at 295 K, μ_{eff} = 17.83 μ_B, per Ho_3; μ_{eff} = 10.31 B.M. per Ho^{3+}.

Crystal Data for 1: $C_{42.60}H_{40.20}GdN_6O_9$ [corresponding to **1**·$(EtOH)_{1.8}(H_2O)_{0.2}$], M = 937.46 g mol^{-1}, monoclinic, $P2_1/c$, a =

9.53390(10) Å, b = 18.9281(3) Å, c = 23.0918(4) Å, β = 93.4862(12)°, V = 4159.40(11) Å^3, Z = 4, $D_{calcd.}$ = 1.497 g cm^3, μ = 1.656 mm^{-1}, T = 123(2) K, θ_{max} = 25.0°, $F(000)$ = 1895, crystal dimensions: 0.18 × 0.14 × 0.13 mm, reflections collected/unique: 45250/7331, R_{int} = 0.0805, final R_1 = 0.0430, wR_2 = 0.1073 [$I > 2\sigma(I)$], GooF = 1.032.

Crystal Data for 2: $C_{79}H_{100}Cl_8Ho_6N_{12}O_{36}$ [corresponding to **2**·$(MeOH)_{0.5}(H_2O)_{5.5}$], M = 3066.89 g mol^{-1}, triclinic, $P\bar{1}$, a = 10.2491(5) Å, b = 17.4612(8) Å, c = 17.8448(11) Å, α = 62.557(2)°, β = 74.375(2)°, γ = 78.991(4)°, V = 2721.1(3) Å^3, Z = 1, $D_{calcd.}$ = 1.872 g cm^3, μ = 4.586 mm^{-1}, T = 123(2) K, θ_{max} = 25.0°, $F(000)$ = 1484, crystal dimensions: 0.11 × 0.11 × 0.09 mm, reflections collected/unique: 24254/9548, R_{int} = 0.1006, final R_1 = 0.0673, wR_2 = 0.1499 [$I > 2\sigma(I)$], GooF = 1.012.

CCDC-697913 (for **1**) and -697914 (for **2**) contain the supplementary crystallographic data for this paper. These data can be obtained free of charge from The Cambridge Crystallographic Data Centre via www.ccdc.cam.ac.uk/data_request/cif.

Supporting Information (see also the footnote on the first page of this article): Plots of isothermal magnetisation, per Gd, for complex **1** (Figure S1) and temperature dependence of the out-of-phase, $\chi_{M''}$, and in-phase, $\chi_{M'}$, (Insert) components of the ac molar magnetic susceptibility of **2** under zero dc field (Figure S2).

Acknowledgments

The authors want to thank Dr. Craig Forsyth (Monash University) for the help provided regarding the crystal structures. This work was supported by the Australian Research Council and Bayer Schering Pharma.

[1] a) R. Wang, Z. Zheng, T. Jin, R. T. Staples, *Angew. Chem. Int. Ed.* **1999**, *38*, 1813–1815; b) D.-S. Zhang, B.-Q. Ma, T.-Z. Jin, S. Gao, C.-H. Yan, T. C. W. Mak, *New J. Chem.* **2000**, *24*, 61–62; c) R. Anwander, *Angew. Chem. Int. Ed.* **1998**, *37*, 599–602; d) D. Freedman, J. H. Melman, T. J. Emge, J. G. Brennan, *Inorg. Chem.* **1998**, *37*, 4162–4163; e) X. Gu, D. Xue, *Inorg. Chem.* **2007**, *46*, 3212–3216; f) G. Gieser, P. Unfried, Z. Zák, *J. Alloys Compd.* **1997**, *257*, 175–181; g) A. Ruiz-Martinez, D. Casanova, S. Alvarez, *Dalton Trans.* **2008**, *19*, 2583–2591.

[2] a) Z. Zheng, *Chem. Commun.* **2001**, 2521–2529; b) A. Babai, A.-V. Mudring, *Z. Anorg. Allg. Chem.* **2006**, *632*, 1956–1958.

[3] a) M. R. Bürgstein, P. W. Roesky, *Angew. Chem. Int. Ed.* **2000**, *39*, 549–551; b) G. B. Deacon, T. Feng, D. C. R. Hockless, P. C. Junk, B. W. Skelton, A. H. White, *Chem. Commun.* **1997**, 341–341; c) G. B. Deacon, G. B. Fallon, C. M. Forsyth, S. C. Harris, P. C. Junk, B. W. Skelton, A. H. White, *Dalton Trans.* **2006**, 802–812; d) G. B. Deacon, C. M. Forsyth, R. Harika, P. C. Junk, J. W. Ziller, W. J. Evans, *J. Mater. Chem.* **2004**, *14*, 3144–3149.

[4] D. M. Lyubov, C. Doring, G. K. Fukin, A. V. Cherkasov, A. S. Shavyrin, R. Kempe, A. A. Trifonov, *Organometallics* **2008**, *27*, 2905–2907.

[5] P. W. Roesky, G. Canesco-Melchor, A. Zulys, *Chem. Commun.* **2004**, *6*, 738–739.

[6] a) T. M. Gamer, Y. Lan, P. W. Roesky, A. K. Powell, R. Clerac, *Inorg. Chem.* **2008**, *47*, 6581–6583; b) N. Mahé, O. Guillou, C. Daiguebonne, Y. Gérault, A. Caneschi, C. Sangregorio, J. Y. Chane-Ching, P. E. Car, T. Roisnel, *Inorg. Chem.* **2005**, *44*, 7743–7750; c) J. Tang, I. Hewitt, N. T. Madhu, G. Chastanet, W. Wernsdorfer, C. E. Anson, C. Benelli, R. Sessoli, A. K. Powell, *Angew. Chem. Int. Ed.* **2006**, *45*, 1729–1733; d) J. Luzon, K. Bernot, I. J. Hewitt, C. E. Hanson, A. K. Powell, R. Sessoli, *Phys. Rev. Lett.* **2008**, *100*, 247205-1 to 247205-4; e) L. F. Chibotaru, L. Ungur, A. Soncini, *Angew. Chem. Int. Ed.* **2008**, *47*, 4126–4129; f) J.-P. Costes, F. Dahan, F. Nicodème, *Inorg. Chem.* **2001**, *40*, 5285–5287.

[7] a) M. K. Thompson, M. Vuchkov, I. A. Kahwa, *Inorg. Chem.* **2001**, *40*, 4332–4341; b) L.-Z. Zhang, W. Gu, B. Li, X. Liu, D.-Z. Liao, *Inorg. Chem.* **2007**, *46*, 622–624; c) R. Wang, D. Song, S. Wang, *Chem. Commun.* **2002**, 368–369.

[8] L. G. Hubert-Pfalzgraf, L. Cauro-Gamet, A. Brethon, S. Daniele, P. Richard, *Inorg. Chem. Commun.* **2007**, *10*, 143–147.

[9] S. V. Eliseeva, O. V. Kotova, F. Gumy, S. N. Semenov, V. G. Kessler, L. S. Lepnev, J.-C. Buenzli, N. P. Kuzmina, *J. Phys. Chem. A* **2008**, *112*, 3614–3626.

[10] a) V. Baskar, P. W. Roesky, *Z. Anorg. Allg. Chem.* **2005**, *631*, 2782–2785; b) V. Baskar, P. W. Roesky, *Dalton Trans.* **2006**, 676–679; c) S. Datta, V. Baskar, H. Li, P. W. Roesky, *Eur. J. Inorg. Chem.* **2007**, 4216–4220.

[11] G. Xu, Z.-M. Wang, Z. He, Z. Lu, C.-S. Liao, C.-H. Yan, *Inorg. Chem.* **2002**, *41*, 6802–6807.

[12] P. C. Andrews, T. Beck, C. M. Forsyth, B. H. Fraser, P. C. Junk, M. Massi, P. W. Roesky, *Dalton Trans.* **2007**, *48*, 5651–5654.

[13] V. Montoya, J. Pons, X. Solans, M. Font-Bardia, J. Ros, *Inorg. Chim. Acta* **2005**, *358*, 2763–2769.

[14] a) P. C. Andrews, C. M. Forsyth, B. H. Fraser, P. C. Junk, M. Massi, M. Silberstein, *CrystEngComm* **2007**, *9*, 282–285; b) T. Fiedler, M. Hilder, P. C. Junk, U. H. Kynast, M. M. Lezhnina, M. Warzala, *Eur. J. Inorg. Chem.* **2007**, 291–301.

[15] a) H. Lueken, P. Hannibal, K. Handrick, *Chem. Phys.* **1990**, 151–161; b) S.-S. Bao, [1].-F. Ma, Y. Wang, L. Fang, C.-J. Zhu, Y.-Z. Li, L.-M. Zheng, *Chem. Eur. J.* **2007**, *13*, 2333–2343.

[16] a) K. R. Lea, M. J. M. Leask, W. P. Wolf, *J. Phys. Chem. Solids* **1962**, *23*, 1381–1405; b) J.-P. Sutter, M. L. Kahn, O. Kahn, *Adv. Mater.* **1999**, *11*, 863–865; c) V. S. Mironov, Y. G. Galyametdinov, A. Ceulemans, C. Görller, K. Binnemans, *J. Chem. Phys.* **2002**, *116*, 4673–4685.

[17] T. C. Bruice, *J. Am. Chem. Soc.* **1957**, *79*, 902–905.

[18] L. M. Wittick, K. S. Murray, B. Moubaraki, S. R. Batten, L. Spiccia, K. J. Berry, *Dalton Trans.* **2004**, 1003–1011.

[19] R. H. Blessing, *J. Appl. Cryst.* **1997**, *30*, 421.

[20] G. M. Sheldrick, *Acta Crystallogr., Sect. A* **2008**, *64*, 112–122.

[21] L. J. Barbour, *J. Supramol. Chem.* **2003**, *1*, 189–191.

Received: October 14, 2008
Published Online: January 14, 2009

